

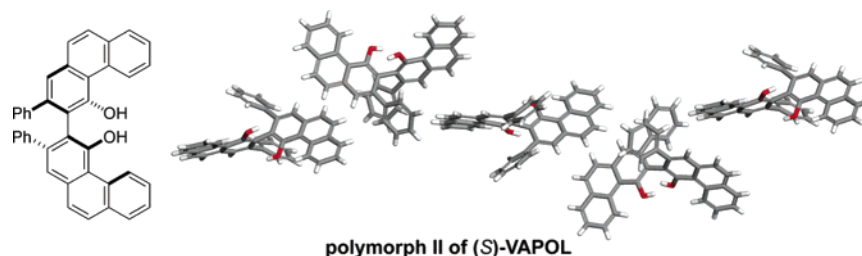
Crystal Chemistry of VAPOL

Christopher P. Price and Adam J. Matzger*

Department of Chemistry and the Macromolecular Science and Engineering Program,
The University of Michigan, Ann Arbor, Michigan 48109-1055

matzger@umich.edu

Received July 6, 2004



Ligands employed in enantioselective catalysis are capable of displaying rich phase behavior that can significantly impact their properties, both structural and physical. To illuminate these issues in a model system, the solid-state structure and properties of the vaulted biaryl ligand VAPOL were investigated. Racemic VAPOL and solvates with toluene and ethyl acetate were structurally characterized. In addition, two polymorphs of (S)-VAPOL were found, and the crystal packing in these and a very stable CH_2Cl_2 solvate was elucidated. In contrast to BINOL, the unsolvated forms of the ligand lack classical hydrogen-bonding motifs. Remarkably, the melting point of racemic VAPOL is 86 °C higher than that of (S)-VAPOL form I, and there is a 2.0 kcal/mol difference in stability at room temperature, favoring the racemate. These values are at the upper end of those observed in the literature for differences between a racemic/chiral pair.

Introduction

Chiral ligands for enantioselective catalysis have become indispensable tools in organic synthesis. These ligands, when complexed to metal centers, allow access to enantioenriched compounds via achiral precursors. Although almost exclusively employed in solution, the solid-state structure of these ligands is nonetheless important because of its role in understanding catalyst structure and controlling solubility during complexation. Significantly, because racemates are often less soluble than enantiopure compounds, enrichment of partially resolved solutions by direct recrystallization can be complicated and often results in decreased recovery.¹ The

presence of polymorphs, multiple crystalline phases of the same molecule each possessing a unique arrangement of these molecules in the solid state, or solvates (pseudopolymorphs) considerably complicates the situation because the solubilities and conformations of the enantiopure compound and/or racemate depend on the specific crystalline form obtained.

Typically, only enantiopure ligands are employed in catalyst formation. However, the racemic compound holds some importance in understanding the chemistry of these systems. In general, a racemic crystal tends to be denser than the corresponding chiral crystal. This phenomenon is known as Wallach's rule and has been subjected to some scrutiny since its first assertion in 1895.^{2–5} In 1991,

(1) Depending on the composition of the eutectic and the ratio of the enantiomers, recrystallization of partially resolved mixtures can provide solids with increased, decreased, or unchanged optical purity: Eliel, E. L.; Wilen, S. H. *Stereochemistry of Organic Compounds*; John Wiley & Sons: New York, 1994; pp 381–387.

(2) Wallach, O. *Liebigs Ann. Chem.* **1895**, 286, 90–143.

(3) Jacques, J.; Collet, A.; Wilen, S. H. *Enantiomers, Racemates, and Resolutions*; John Wiley & Sons: New York, 1981; pp 23–31.

(4) Brock, C. P.; Schweizer, W. B.; Dunitz, J. D. *J. Am. Chem. Soc.* **1991**, 113, 9811–9820.

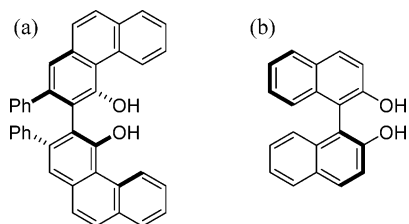


FIGURE 1. (a) Structure of (*S*)-VAPOL. (b) Structure of (*S*)-BINOL.

Brock, Schweizer, and Dunitz conducted a Cambridge Structural Database (CSD) search of chiral compounds to test the accuracy of this rule. This study found that for resolvable enantiomers, on average, racemic crystals are 1% more tightly packed than their chiral counterparts. Furthermore, it is found that crystallization from a racemic solution or melt usually produces a racemate instead of a 1:1 mixture of the crystals of both enantiomers.⁶

Although no unified theory connecting molecular parameters such as the extent of chirality with differences between the properties of racemic and enantiopure solids exists, one might expect that differences are more pronounced for molecules possessing highly dissymmetric configurations, such as ligands commonly used in enantioselective catalysis. One metric for chirality, introduced by Ferrarini and Nordio and applied to assess the molecular chirality of some biaryls on the basis of molecular shape, is the helicity tensor.⁷ In the cases of biphenyl, 1,1'-binaphthyl, and 1,1'-bianthryl, the magnitude of this chirality measure increases in this series from biphenyl to bianthryl. To explore the possibility that a highly chiral molecule may display large differences in properties between enantiopure and racemic material, we scrutinized the solid-state chemistry of the vaulted biaryl ligand 2,2'-diphenyl-[3,3'-biphenanthrene]-4,4'-diol (VAPOL, Figure 1a).⁸ This ligand, which contains a helical arrangement of phenyl-substituted phenanthrene units, functions with extraordinary efficiency in enantioselective catalysis and has been utilized as the key component of several asymmetric catalysts employed in Diels–Alder,^{9–11} imino aldol,¹² and aziridination^{13–15} reactions. Furthermore, it often displays a greater selectivity than other well-studied biaryl catalysts, such as 2,2'-dihydroxy-1,1'-binaphthyl (BINOL, Figure 1b).^{9,10,12–15}

(5) Eliel, E. L.; Wilen, S. H. *Stereochemistry of Organic Compounds*; John Wiley & Sons: New York, 1994; pp 165–167.

(6) Jacques, J.; Collet, A.; Wilen, S. H. *Enantiomers, Racemates, and Resolutions*; John Wiley & Sons: New York, 1981; p 81.

(7) Ferrarini, A.; Nordio, P. L. *J. Chem. Soc., Perkin Trans. 2* **1998**, 455–460.

(8) Bao, J. M.; Wulff, W. D.; Dominy, J. B.; Fumo, M. J.; Grant, E. B.; Rob, A. C.; Whitcomb, M. C.; Yeung, S. M.; Ostrander, R. L.; Rheingold, A. L. *J. Am. Chem. Soc.* **1996**, *118*, 3392–3405.

(9) Bao, J. M.; Wulff, W. D.; Rheingold, A. L. *J. Am. Chem. Soc.* **1993**, *115*, 3814–3815.

(10) Bao, J. M.; Wulff, W. D. *Tetrahedron Lett.* **1995**, *36*, 3321–3324.

(11) Heller, D. P.; Goldberg, D. R.; Wulff, W. D. *J. Am. Chem. Soc.* **1997**, *119*, 10551–10552.

(12) Xue, S.; Yu, S.; Deng, Y. H.; Wulff, W. D. *Angew. Chem., Int. Ed.* **2001**, *40*, 2271–2274.

(13) Antilla, J. C.; Wulff, W. D. *J. Am. Chem. Soc.* **1999**, *121*, 5099–5100.

(14) Antilla, J. C.; Wulff, W. D. *Angew. Chem., Int. Ed.* **2000**, *39*, 4518–4521.

(15) Loncaric, C.; Wulff, W. D. *Org. Lett.* **2001**, *3*, 3675–3678.

Results and Discussion

Although crystallographic data on uncomplexed VAPOL were not known, it rapidly became apparent that large differences between molecular packing in the racemic and enantiopure crystals must exist. Racemic VAPOL melts at a temperature 86 °C higher than (*S*)-VAPOL (form I, *vide infra*). This is at the upper end of the values found in the literature for melting point differences between a racemic/chiral pair.^{16,17} To measure the crystal stability difference giving rise to this effect, the relative free energies of the racemic and enantiopure crystals were determined from their solubility differences. In fact, (*S*)-VAPOL is 30(2) times more soluble than *rac*-VAPOL (solubility measurements were performed in heptane; see Experimental Section). This equates to a relative free-energy difference of 2.00(3) kcal/mol, with *rac*-VAPOL being more stable.¹⁸ In this context, it is interesting to note that in a compilation by Leclercq, Collet, and Jacques¹⁹ for 36 pairs of racemates and enantiomers it was found that melting-point differences can be correlated to differences in the free energy of the pair. In their study, for the largest difference in melting point of a pair (80.5 °C), there is a free-energy difference of 1.7 kcal/mol. For reference, other biaryl compounds such as BINOL and 2,2'-dibromo-1,1'-binaphthyl display differences in melting points of 8 and 30 °C, respectively.

To gain insight into the factors leading to the stabilization of the racemic crystals, crystal structures of racemic

(16) For examples of ≥ 30 °C differences in the melting points between enantiomer and racemate pairs, see: (a) Birnbaum, S. M.; Levintow, L.; Kingsley, R. B.; Greenstein, J. P. *J. Biol. Chem.* **1952**, *194*, 455–470. (b) Fredga, A.; Matell, M. *Bull. Soc. Chim. Belg.* **1953**, *62*, 47–54. (c) Armarego, W. L. F.; Turner, E. E. *J. Chem. Soc.* **1957**, 13–22. (d) Clark-Lewis, J. W.; Roux, D. G. *J. Chem. Soc.* **1959**, 1402–1406. (e) Suszko, J.; Kielczewski, M. *Roc. Chem.* **1967**, *41*, 1291–1302. (f) Leclercq, M.; Collet, A.; Jacques, J. *Tetrahedron* **1976**, *32*, 821–828. (g) Kuroda, R.; Mason, S. F. *J. Chem. Soc., Perkin Trans. 2* **1981**, 870–876. (h) Chickos, J. S.; Garin, D. L.; Hitt, M.; Schilling, G. *Tetrahedron* **1981**, *37*, 2255–2259. (i) Brown, K. J.; Berry, M. S.; Murdoch, J. R. *J. Org. Chem.* **1985**, *50*, 4345–4349. (j) Simon, K.; Acs, M.; Larsen, S.; Fülöp, V.; Gács-Baitz, E. *Acta Crystallogr., Sect. B: Struct. Sci.* **1992**, *48*, 88–95. (k) Duddu, S. P.; Grant, D. J. W. *Pharm. Res.* **1992**, *9*, 1083–1091. (l) Wearley, L.; Antonacci, B.; Cacciapuoti, A.; Assenza, S.; Chaudry, I.; Eckhart, C.; Levine, N.; Loebenberg, D.; Norris, C.; Parmegiani, R.; Sequeira, J.; Yarosh-Tomaine, T. *Pharm. Res.* **1993**, *10*, 136–140. (m) Neau, S. H.; Shinwari, M. K.; Hellmuth, E. W. *Int. J. Pharm.* **1993**, *99*, 303–310. (n) Tamura, R.; Ushio, T.; Takahashi, H.; Nakamura, K.; Azuma, N.; Toda, F.; Endo, K. *Chirality* **1997**, *9*, 220–224. (o) Li, Z. J.; Zell, M. T.; Munson, E. J.; Grant, D. J. W. *J. Pharm. Sci.* **1999**, *88*, 337–346. (p) Ros, F.; Molina, M. T. *Eur. J. Org. Chem.* **1999**, 3179–3183. (q) Wang, X.; Wang, X. J.; Ching, C. B. *Chirality* **2002**, *14*, 318–324. (r) Roux, M. V.; Jiménez, P.; Vacas, A.; Cano, F. H.; Apreda-Rojas, M. D.; Ros, F. *Eur. J. Org. Chem.* **2003**, 2084–2091.

(17) A 200 °C difference in melting points has been observed for a derivative of *o*-tetraphenylene: Rajca, A.; Safronov, A.; Rajca, S.; Wongsriratanakul, J. *J. Am. Chem. Soc.* **2000**, *122*, 3351–3357. Although the enantiopure compound forms crystals containing acetonitrile guests, its melting behavior by differential scanning calorimetry is glasslike, with a glass transition temperature of about 213 °C; the racemate has the usual crystalline melting point at about 430 °C. In addition, the enantiopure compound readily forms isotropic films of good optical quality. Thus, this comparison of melting behavior is between enantiopure glass and racemic crystal: Andrzej Rajca, personal communication.

(18) The stability differences were calculated from UV–visible absorbance by the equation $\Delta G = RT \ln K$, with $K = [(\text{S})\text{-VAPOL absorbance}]/[\text{rac-VAPOL absorbance}]$. The free-energy difference was calculated for each of the three wavelength maxima, and these values were averaged to give the final free-energy difference.

(19) Jacques, J.; Collet, A.; Wilen, S. H. *Enantiomers, Racemates, and Resolutions*; John Wiley & Sons: New York, 1981; pp 93–100.

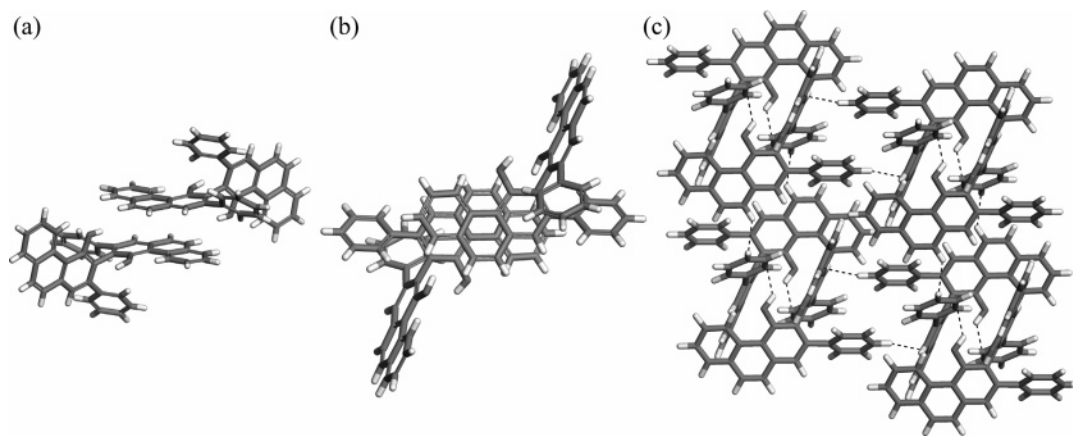


FIGURE 2. (a) Side-on view of a π -stacked dimer in *rac*-VAPOL (approximately looking down the *b*-axis). (b) View orthogonal to the π -stacked dimer in *rac*-VAPOL. (c) View along the *a*-axis of a sheet of *rac*-VAPOL molecules. Intermolecular interactions discussed in the text are represented with dashed lines.

and enantiopure VAPOL were determined. Remarkably, during routine crystallization studies, the crystal structures of three VAPOL solvates were obtained as well as three unsolvated forms of VAPOL; in addition to the *rac*-VAPOL and the (*S*)-VAPOL form I discussed above, a second form of (*S*)-VAPOL, dubbed form II, was discovered. The data indicate that one polymorph of (*S*)-VAPOL obeys Wallach's rule, although the other is an exception. *rac*-VAPOL is more dense than (*S*)-VAPOL form II, but (*S*)-VAPOL form I is slightly more dense than *rac*-VAPOL. In solution, the less-dense polymorph of (*S*)-VAPOL converts to the more-dense polymorph, indicating that form I has the lowest free energy. The dihedral angles between the phenanthrenes observed in these structures are all $<90^\circ$ (cisoid conformation²⁰). These angles vary from 80.1, 87.9, and 88.5° in (*S*)-VAPOL form I (three inequivalent molecules, *vide infra*) and 73.0° in (*S*)-VAPOL form II to 78.6° in *rac*-VAPOL, indicating some flexibility about the biaryl bond. As expected, binding the oxygens to a central atom further reduces the dihedral angle, as seen in the phosphoric amide complex ($\sim 58^\circ$).⁹

Racemic VAPOL crystallizes in space group $P\bar{1}$, with two molecules in the unit cell (one of each enantiomer) related by an inversion center. Parts a and b of Figure 2 depict the packing of one π dimer formed between enantiomers. The view, orthogonal to the stacked phenanthrenes, reveals the considerable overlap between the π systems at approximately 3.4 Å. The packing structure is characterized by sheets of VAPOL molecules that are formed by O–H $\cdots\pi$ and two different C–H $\cdots\pi$ interactions (Figure 2c). These occur between a hydroxyl and a phenyl ring at a normalized bond distance²¹ and angle of 2.49 Å and 131°, a phenyl to a phenanthrene at 2.69 Å and 160°, and a phenanthrene to a carbon on a phenyl ring at 2.65 Å and 136°, respectively. Adjacent sheets are

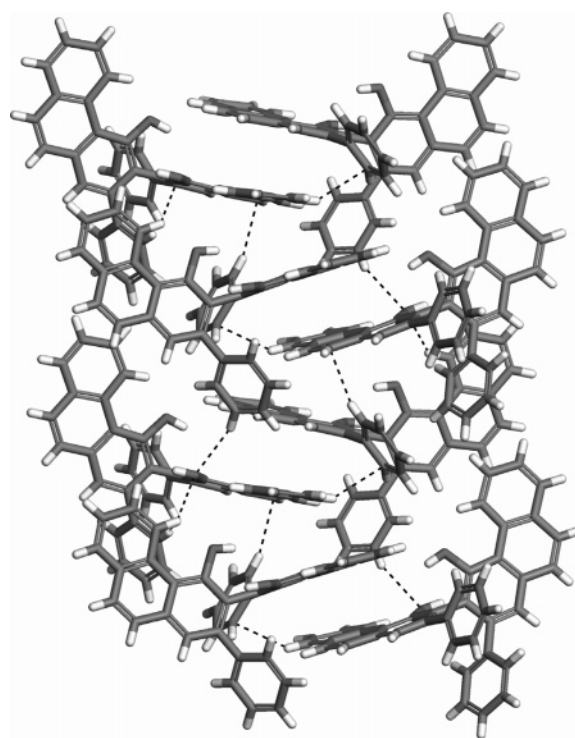


FIGURE 3. Chain of π dimers in (*S*)-VAPOL form I stacked parallel to the *b*-axis with C–H $\cdots\pi$ and C–H \cdots O intermolecular interactions highlighted (viewed along the *a*-axis).

linked by π stacks of phenanthrene units. Surprisingly, no intermolecular or intramolecular hydrogen bonding involving the hydroxyl groups as acceptors occurs in this structure.

(*S*)-VAPOL exists in two solvent-free polymorphs that, although possessing different molecular-packing arrangements, each has an extended helical arrangement of molecules. Polymorph I crystallizes in the orthorhombic space group $P2_12_12_1$, with three crystallographically inequivalent molecules and 12 molecules total in the unit cell. In contrast to *rac*-VAPOL, form I of (*S*)-VAPOL possesses infinite chains of slipped $\pi\cdots\pi$ dimers (stacking distance of 3.46 Å) that are connected by C–H $\cdots\pi$ and two different C–H \cdots O interactions (Figure 3). The

(20) The terms *cisoid* and *transoid* describe biaryl dihedral angles of $<90^\circ$ and $>90^\circ$, respectively: (a) Kerr, K. A.; Robertson, J. M. *J. Chem. Soc. B* **1969**, 1146–1149. (b) Kress, R. B.; Duesler, E. N.; Etter, M. C.; Paul, I. C.; Curtin, D. Y. *J. Am. Chem. Soc.* **1980**, *102*, 7709–7714. (c) Kuroda, R.; Mason, S. F. *J. Chem. Soc., Perkin Trans. 2* **1981**, 167–170. (d) Pu, L. *Chem. Rev.* **1998**, *98*, 2405–2494.

(21) The carbon–hydrogen and oxygen–hydrogen bond lengths in all of the structures were normalized to 1.083 and 0.983 Å, respectively, before analysis.

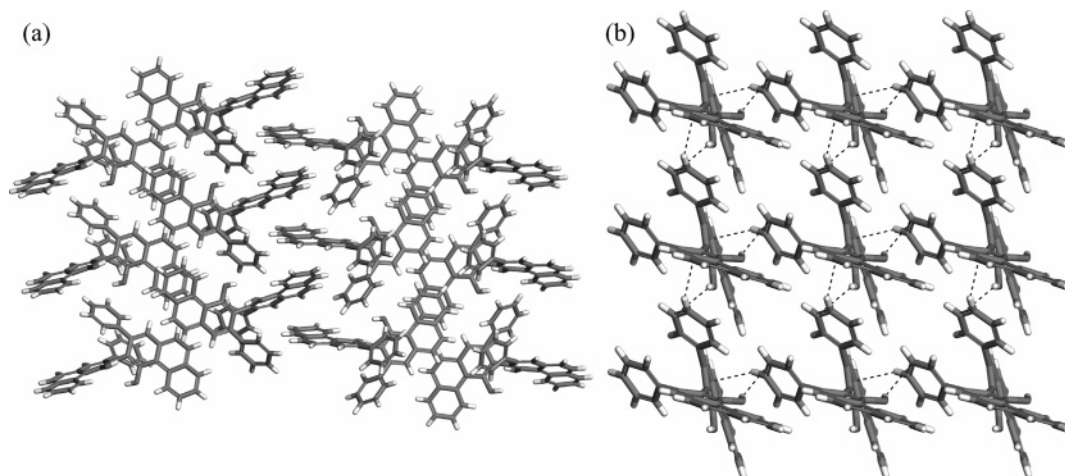


FIGURE 4. (a) Packing diagram viewed down the a -axis of (*S*)-VAPOL form II, depicting the interdigitated phenanthrenes between two neighboring chains. (b) View down the c -axis in (*S*)-VAPOL form II, revealing a sheet of VAPOL molecules.

C–H $\cdots\pi$ bond occurs from a phenyl to a phenanthrene with a bond length of 2.65 Å and an angle of 159°, while the C–H \cdots O interactions couple a phenyl to a hydroxyl and a phenanthrene to the same hydroxyl at 2.60 Å (151°) and 2.59 Å (124°), respectively. The chains of the π dimers are laterally connected by several C–H $\cdots\pi$, C–H \cdots O, and van der Waals interactions, which link this motif into the three-dimensional network. Form II of (*S*)-VAPOL exists in tetragonal space group $P4_32_12$. A 4_3 screw axis gives rise to a corkscrew arrangement of molecules (Figure 4a). Sheets of VAPOL molecules are held together by C–H $\cdots\pi$ and O–H $\cdots\pi$ interactions, with the latter occurring from a hydroxyl to a nearby phenyl with a bond distance of 2.65 Å and an angle of 146° and the former taking place from the same phenyl to a phenanthrene at a distance and angle of 2.62 Å and 148°, respectively (Figure 4b). The two-dimensional sheets are connected through van der Waals interactions by interdigitated phenanthrenes. The main structural differences between the two polymorphs of (*S*)-VAPOL lay in the infinite $\pi\cdots\pi$ dimer stacks in form I and the C–H $\cdots\pi$ and O–H $\cdots\pi$ interactions in form II. Each forms two-dimensional nets of molecules, albeit, through different types of close contacts that are linked by directional interactions in form I and van der Waals contacts in form II.

Despite possessing both strong hydrogen bond donors and acceptors, the three solvent-free structures of VAPOL show no classical hydrogen bonds. Other biaryl ligands, in fact, do form these types of hydrogen bonds. In the case of BINOL, hydrogen bonding occurs in both the enantiopure and racemic crystal structures.^{22,23} These interactions give rise to a helical arrangement of BINOL molecules down a 3_2 screw axis in the homochiral structure and a 2_1 screw axis in the racemic case. In both structures, these helices are connected by classical intermolecular hydrogen bonding that is mediated by hydroxyl donors and acceptors. The dihedral angle between the naphthalenes of both structures of BINOL is

>90° (transoid conformation²⁰). This condition essentially exposes the hydroxyl functionality making hydrogen bonding more feasible. However, in VAPOL, all structures are in the cisoid conformation, which radically alters the preferred packing motif. Moreover, in VAPOL, the hydroxyls are buried in the pocket created by the phenanthrene portions of the molecule, and the steric repulsion of these groups discourages possible hydrogen bonding. This is not the case for BINOL because its hydroxyls are exposed on the outside of the molecule, and this, along with its transoid conformation, allows for hydrogen bonding to occur. It appears that in VAPOL, the combined C–H $\cdots\pi$, O–H $\cdots\pi$, and $\pi\cdots\pi$ interactions, as well as van der Waals contacts in the adopted arrangement, are more energetically favored than packing patterns satisfying classical hydrogen bonding.

As important as polymorphism is in determining the stability, solubility, and dissolution rate of a given compound, the inclusion of solvent in the lattice can exert even greater effects. In the course of crystallization studies from a diverse array of solvents, three pseudopolymorphs of VAPOL were identified and structurally characterized: a toluene solvate of *rac*-VAPOL, an ethyl acetate solvate of *rac*-VAPOL, and an (*S*)-VAPOL CH_2Cl_2 solvate (see Supporting Information). The toluene solvate of *rac*-VAPOL crystallized in $P\bar{1}$, with one toluene and two VAPOL molecules in the unit cell. The packing arrangement accommodates columns of disordered toluene guests separated by pairs of phenyl rings from the VAPOL. Thermogravimetric analysis (TGA)²⁴ of the *rac*-VAPOL toluene solvate indicates a mass loss at 117 °C, the magnitude of which is consistent with the loss of toluene from the crystal. The ethyl acetate solvate crystallizes in $P\bar{1}$, with two VAPOL molecules in the unit cell and one disordered ethyl acetate. The solvent molecule is trapped in a cage formed by VAPOL molecules in an arrangement to accommodate an OH hydrogen bond donation from VAPOL to the solvent molecule. TGA shows a mass loss at 149 °C that results from the

(22) Mori, K.; Masuda, Y.; Kashino, S. *Acta Crystallogr., Sect. C: Cryst. Struct. Commun.* **1993**, *49*, 1224–1227.

(23) Toda, F.; Tanaka, K.; Miyamoto, H.; Koshima, H.; Miyahara, I.; Hirotsu, K. *J. Chem. Soc., Perkin Trans. 2* **1997**, 1877–1885.

(24) All experiments were performed on a TA Instruments Q500 TGA, and the samples were heated from 25 to 700 °C at 5 °C/min using 5–10 mg of solvated crystals.

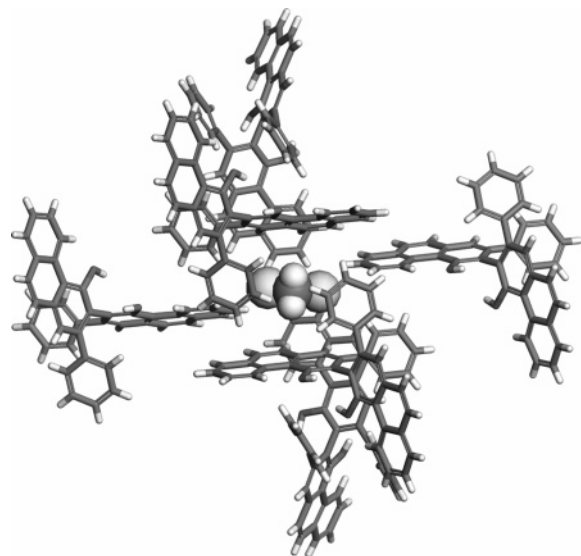


FIGURE 5. (*S*)-VAPOL CH_2Cl_2 solvate showing a pocket created by VAPOL ligands (stick representation) encapsulating a space-filled CH_2Cl_2 molecule.

expulsion of ethyl acetate from the crystals. Because the boiling point of ethyl acetate is much lower than that of toluene, the higher temperature of desolvation for the former is, perhaps, unexpected. However, this difference is consistent with the notion that hydrogen bonding present in the ethyl acetate solvate is relatively strong and suppresses solvent loss.

The (*S*)-VAPOL CH_2Cl_2 solvate crystallizes in trigonal space group $P\bar{3}21$. Its unit cell contains three CH_2Cl_2 and six (*S*)-VAPOL molecules. Solvent molecules are trapped in pockets formed by $\text{C-H}\cdots\pi$ interactions between phenyl donors and phenanthrene acceptors (Figure 5). Because the solvent is unable to leave without substantial reorganization of the VAPOL molecules, desolvation proceeds at a relatively high temperature (179 °C), determined by TGA analysis. This temperature is higher than that required for desolvation of either *rac*-VAPOL form, despite the much lower boiling point of CH_2Cl_2 : a likely indication that the greater lattice stability of the racemic crystals is playing a role in determining the kinetics of solvent loss.

Conclusion

The critical role of crystal form in determining the properties of chiral ligands has been demonstrated for VAPOL. The most dramatic changes are observed between racemic and enantiopure crystal forms. However, as in the case of pigments and pharmaceuticals, the presence of polymorphism must be taken into account in order to fully understand the solid-state chemistry of the system. The differences in melting point and solubility between enantiopure and racemic VAPOL are at the very upper end of values observed in organic compounds. This may be a manifestation of the highly chiral conformation of the VAPOL ligand. However, dissecting the importance of this factor will require both the collection of an appropriate set of reference data and the application of a suitable chirality metric.²⁵ In contrast to other phenol-containing biaryl ligands, classical hydrogen bonds

are absent in all three of the crystal structures of unsolvated VAPOL. Differences, instead, arise from relatively subtle changes in packing arrangement, changes that in aggregate cause considerable modifications in crystal stability.

Experimental Section

Crystal Growth. Solvent-free racemic VAPOL was produced from the ethyl acetate solvate by heating the solvated crystals in phenyl octane to 195 °C followed by cooling the mixture at a rate of 15 °C/min. Small platelike crystals suitable for single-crystal X-ray diffraction formed below 120 °C. (*S*)-VAPOL form I crystals were grown by boiling the CH_2Cl_2 solvate in heptane at 105 °C, which produced platelike crystals. (*S*)-VAPOL form II crystals were produced by heating the CH_2Cl_2 solvate from 100 to 150 °C at a rate of 20 °C/min in 2,2,4,4,6,8,8-heptamethylnonane. The crystals partially dissolved at 140 °C, and small octahedral crystals grew. Single crystals of the ethyl acetate solvate of *rac*-VAPOL were produced by cooling a 6.2 mg/mL solution in ethyl acetate from 60 °C in a sealed vial. Small crystals of rodlike morphology formed from solution over several days. *rac*-VAPOL toluene solvate crystals were formed by adding 1 mL of toluene to 8 mg of the ethyl acetate solvate and by heating the mixture to 70 °C followed by slow cooling to yield blocklike crystals. Single crystals of the CH_2Cl_2 solvate of (*S*)-VAPOL were produced by dissolving 4.6 mg of the CH_2Cl_2 solvate in 1 mL of a 9:1 hexanes/ CH_2Cl_2 mixture and allowing this solution to evaporate at room temperature over several days. This produced prism-shaped crystals.

Thermomicroscopy. All thermomicroscopy was performed with a Mettler Toledo FP82HT hot stage connected to an FP 90 control processor and viewed under cross-polarized light with a Leica DMLP microscope. Solvent-free *rac*-VAPOL crystals were heated from 310 to 320 °C at a rate of 1 °C/min. These melted from 312 to 313.2 °C. Crystals of solvent-free (*S*)-VAPOL form I and form II were heated side by side from 220 to 235 °C at a rate of 1 °C/min. Small cracks formed in the crystal of form II, indicating a phase change, and both crystals melted from 226.2 to 227.9 °C.

Solubility Measurements. These experiments were carried out on a Cary 300 Bio UV–visible spectrophotometer at room temperature. Solvent-free *rac*-VAPOL and (*S*)-VAPOL crystals were placed in separate 4 mL vials, and 3 mL of heptane was added to each. These vials were heated to 35 °C for 2 h, cooled to room temperature, and left to equilibrate for 3 days. A solid was observed at the bottom of each vial, indicating that the solutions were saturated. Aliquots of each solution (1.00 mL) were diluted to 10.0 mL for *rac*-VAPOL and 100 mL for (*S*)-VAPOL due to their differences in solubility. This solution was added to quartz cuvettes, and the absorbance was measured between 220 and 800 nm.

Single-Crystal X-ray Diffraction. All intensity data were collected at –120 °C on a Bruker SMART CCD diffractometer with graphite monochromated Mo K α ($\lambda = 0.71073$ Å) radiation. *rac*-VAPOL, *rac*-VAPOL toluene solvate, *rac*-VAPOL ethyl acetate solvate, (*S*)-VAPOL form I, and (*S*)-VAPOL CH_2Cl_2 solvate structures were solved and refined using the Bruker SHELXTL software package.²⁶ (*S*)-VAPOL form II was solved using SIR 2002²⁷ and refined using SHELX97 within

(25) Although there is no unique way to define the extent of chirality for a given molecule, generally applicable schemes are outlined in ref 7 and in the following: Zabrodsky, H.; Avnir, D. *J. Am. Chem. Soc.* **1995**, *117*, 462–473.

(26) Sheldrick, G. M. *SHELXTL*, version 6.14; Bruker Analytical X-ray: Madison, WI, 2000.

(27) Burla, M. C.; Camalli, M.; Carrozzini, B.; Cascarano, G. L.; Giacovazzo, C.; Polidori, G.; Spagna, R. *J. Appl. Crystallogr.* **2003**, *36*, 1103.

WinGX version 1.64.05.²⁸ All non-hydrogen atoms were refined anisotropically with C–H hydrogen atoms generated at idealized positions and refined as riding atoms with individual isotropic displacement parameters. Hydrogen atoms attached to oxygens were generated at idealized positions, refined as riding atoms with individual isotropic displacement parameters, and allowed to rotate about the C–O bond.

Acknowledgment. This work was supported by SSCI Inc. and the Beckman Foundation. We are grateful

to Professor William Wulff for VAPOL samples and Professor Omar Yaghi for the use of his diffractometer.

Supporting Information Available: Packing diagrams for *rac*-VAPOL toluene and ethyl acetate solvates. The thermal ellipsoid plots and the crystallographic information files for *rac*-VAPOL, (*S*)-VAPOL form I, (*S*)-VAPOL form II, *rac*-VAPOL toluene solvate, *rac*-VAPOL ethyl acetate solvate, and (*S*)-VAPOL CH₂Cl₂ solvate are given. This material is available free of charge via the Internet at <http://pubs.acs.org>.

(28) Farrugia, L. J. *J. Appl. Crystallogr.* **1999**, *32*, 837–838.

JO048853N